Multiple Roles of Arginine 181 in Binding and Catalysis in the NAD-Malic Enzyme from *Ascaris suum*†

William E. Karsten and Paul F. Cook*

Department of Chemistry and Biochemistry, University of Oklahoma, 620 Parrington Oval, Norman, Oklahoma 73019

Received July 31, 2007; Revised Manuscript Received October 2, 2007

ABSTRACT: The NAD-malic enzyme catalyzes the oxidative decarboxylation of L-malate. Structures of the enzyme indicate that arginine 181 (R181) is within hydrogen bonding distance of the 1-carboxylate of malate in the active site of the enzyme and interacts with the carboxamide side chain of the nicotinamide ring of NADH, but not with NAD^+. Data suggested R181 might play a central role in binding and catalysis in malic enzyme, and it was thus changed to lysine and glutamine to probe its potential function. A nearly 100-fold increase in the K_m for malate and a 30-fold increase in the K_i for oxalate, an analogue of the enolpyruvate intermediate, in the R181Q and R181K mutants are consistent with a role for R181 in binding substrates. The mutant enzymes also exhibit a >10-fold increase in K_{iNADH}, but only a slight or no change in K_{NAD}, consistent with rotation of the nicotinamide ring into the malate binding site upon reduction of NAD^+ to NADH. The activity of the R181Q mutant can be rescued by ammonium ion likely by binding in the pocket vacated by the guanidinium group of R181. Results suggest 2 mol of ammonia bind per mole of active sites with a high-affinity K_{NH4} of 0.7 ± 0.1 mM and a low-affinity K_{NH4} of ∼420 mM. Occupancy of the high-affinity site, likely by NH_4^+, results in an increase in the affinity of malate, oxalate, and NADH (with no change in NAD affinity), consistent with the above-proposed roles for R181. The second molecule to bind is likely neutral NH_3, and its binding increases V/E_t ∼20-fold. Primary deuterium and ^{13}C isotope effects measured in the absence and presence of ammonium ion suggest R181Q predominantly affects the rate of the reaction by changing the rate of the precatalytic conformational change. The isotope effects do not change upon binding the second mole of ammonia in spite of the 20-fold increase in V/E_t. Thus, the R181Q mutant enzyme exists as an equilibrium mixture between active and less active forms, and NH_3 stabilizes the more active conformation of the enzyme.

The mitochondrial nicotinamide adenine dinucleotide-malic enzyme (EC 1.1.139) from *Ascaris suum* catalyzes the divalent metal ion-dependent oxidative decarboxylation of L-malate utilizing NAD^1 to yield CO_2, pyruvate, and NADH. The kinetic mechanism of the enzyme is random with respect to NAD and malate; however, the divalent metal ion must bind prior to malate (*1*). With NAD as the dinucleotide substrate, the chemical mechanism is stepwise with hydride transfer from malate to NAD preceding decarboxylation of the oxaloacetate intermediate (*2*−*4*). The divalent metal ion acts as a Lewis acid to assist decarboxylation of oxaloacetate. The intrinsic ^{13}C isotope effect on the decarboxylation step is ∼1.052, similar to the value of 1.05 for the nonenzymatic decarboxylation of oxaloacetate catalyzed by several different metal ions, and suggests similar late transition states for the enzymatic and nonenzymatic catalyzed decarboxylation of oxaloacetate (*4*, *5*). The estimated intrinsic primary deuterium isotope effect for hydride transfer in the NAD-malic enzyme reaction is 11, greater than the semiclassical limit, and suggests a tunneling contribution to this step. The possibility of tunneling in the hydride transfer step was later supported by the α-secondary tritium isotope effect, which suggested tunneling and coupling of the motion of the hydride and the secondary hydrogens in the reaction coordinate for the hydride transfer step (*6*). A number of active site residues implicated in catalysis have been subjected to site-directed mutagenesis studies and lead to the proposal of a catalytic triad involving Y126, K199, and D294 (*7*). Little has been done to characterize the role of residues involved in binding substrates and their contribution to catalysis.

There are currently a number of crystal structures of malic enzyme from different sources with ligands bound (*8*−*11*). The enzyme is a tetramer composed of a dimer of dimers. When malate binds, there is significant closure of the active site. In the human enzyme, a closed structure of a complex with malate, NADH, and Mg^{2+} shows that arginine 165 is within hydrogen bonding distance of the α-carboxyl of malate, one of the oxygens of the pyrophosphyl moiety of NADH, and the backbone carbonyl oxygen of leucine 167 (*10*). The homologous residues in the *Ascaris* enzyme are arginine 181 and leucine 183. These interactions are depicted in Figure 1A using the *A. suum* numbering scheme. However,

† This work was supported by a grant to P.F.C. from the National Science Foundation (MCB 0091207) and the Grayce B. Kerr endowment to the University of Oklahoma to support the research of P.F.C.

* To whom correspondence should be addressed. Telephone: (405) 325-4581. Fax: (405) 325-7182. E-mail: pcook@ou.edu.

[1] Abbreviations: Ches, 2-(*N*-cyclohexylamino)-1-ethanesulfonic acid; Hepes, *N*-(2-hydroxyethyl)piperazine-*N*′-2-ethanesulfonic acid; NAD, nicotinamide adenine dinucleotide (the positive charge is omitted for convenience); NADH, reduced nicotinamide adenine dinucleotide; Pipes, piperazine-*N*,*N*′-bis(2-ethanesulfonic acid); SE, standard error; TDH, tartrate dehydrogenase; Gdn, guanidinium.

10.1021/bi701524z CCC: $37.00
Published on Web 11/21/2007

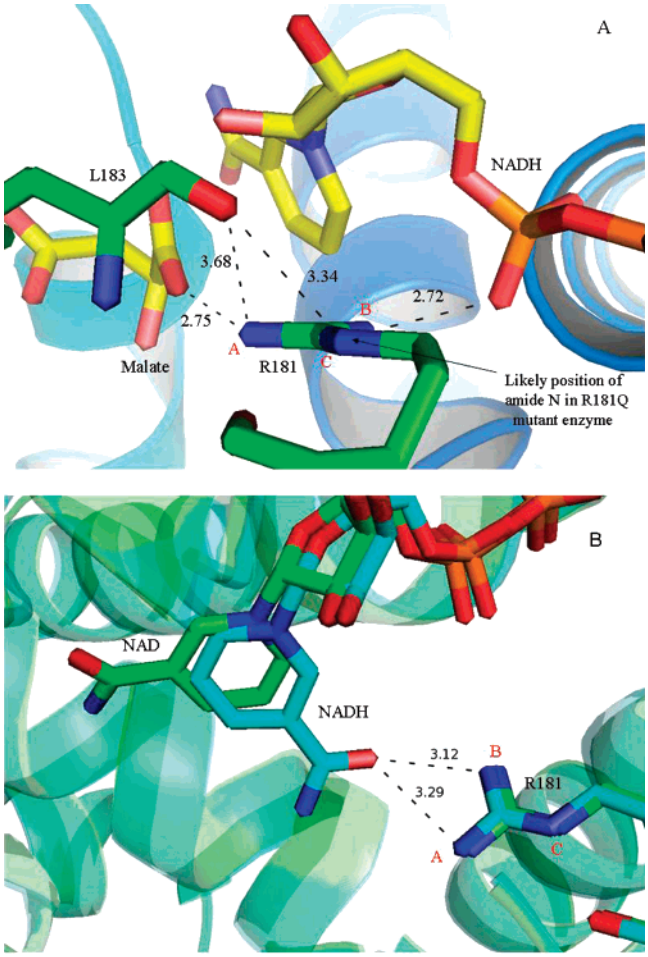

FIGURE 1: (A) Close-up view of the active site of human malic enzyme (PDB entry 1PJ2) in complex with malate and NADH showing the interactions of R181 with malate, NADH, and L183. The amino acid numbering scheme is for the *A. suum* enzyme. The dashed lines represent likely hydrogen bonds, and the numbers indicate the distance Å. The likely position of the amide N in the R181Q mutant enzyme is indicated in the figure, and the guanidinium nitrogens of R181 are labeled A, B, and C for reference in the text. (B) Superposition of the structures of the *A. suum* malic enzyme in complex with either NAD or NADH showing the >180° rotation of the nicotinamide ring of NADH compared to NAD. The dashed lines indicate likely hydrogen bonds between R181 and the nicotinamide ring of NADH, and the numbers represent distances Å. The PDB entries are 1llQ for the NAD structure and 1O0S for the NADH structure. The figures were created using PyMOL from DeLano Scientific LLC (www.pymol.com).

in open structures of the *Ascaris* enzyme with either NAD or NADH bound, R181 is more than 4 Å from the pyrophosphate oxygen of NAD(H) and the carbonyl oxygen of leucine 183 is rotated away from R181 and does not interact with it. Binding of malate likely closes the site and leads to the formation of the interactions shown in Figure 1A. Arginine 181 forms critical interactions that link both of the substrates and the enzyme. A structure of the *Ascaris* enzyme in complex with NADH reveals there is >180° rotation of the nicotinamide ring around the *N*-glycosidic bond compared to its position with NAD bound (Figure 1B) (*8*, *9*). The new position of the reduced nicotinamide overlaps the malate binding site. In the NADH structure, the carboxamide side chain of the nicotinamide ring is within hydrogen bonding distance of R181. In contrast, no interaction of R181 with the nicotinamide ring of NAD is observed. In 6-phosphogluconate dehydrogenase, an enzyme that catalyzes a reaction similar to malic enzyme, a similar rotation of the nicotinamide ring is observed and the ring flip has been implicated as being important in catalysis (*12*−*14*).

Considering the potential multiple roles of arginine 181 in binding malate, the oxidized and reduced dinucleotide substrates, and the possible role of R181 in linking the substrates to the protein and closure of the active site, site-directed mutagenesis to mutate R181 to either lysine or glutamine was conducted. The mutant enzymes were completely characterized, and the results are discussed in the context of the mechanism of the malic enzyme.

MATERIALS AND METHODS

Chemicals. L-Malate was obtained from Sigma, while pyruvate, NAD, and NADH were obtained from either Sigma or USB. Magnesium sulfate, manganese sulfate, and ammonium chloride were from Fisher. Ammonium sulfate was purchased from Amresco. Hepes, Ches, and Pipes buffers were from Research Organics. Sodium borodeuteride (98 at. %) was purchased from Aldrich. The QuikChange site-directed mutagenesis kit was from Stratagene. The recombinant *A. suum* malic enzyme used in these studies has an N-terminal six-histidine tag, and the mutant enzymes were prepared and purified as described previously (*15*). Protein concentrations were estimated using the method of Bradford (*16*).

Synthesis of L-Malate-2-d. L-Malate-2-*d* was synthesized by the reduction of oxaloacetate with sodium borodeuteride. Oxaloacetate (2.6 g) was dissolved in 200 mL of H_2O and the pH adjusted to 7 with KOH. Sodium borodeuteride (0.7 g) was added to the oxaloacetate solution and the mixture allowed to incubate at room temperature for at least 1 h. The pH was adjusted to 5 with acetic acid and the mixture incubated for ~30 min. Solid Pipes buffer and NAD were added to give final concentrations of 25 and 0.2 mM, respectively. The pH was adjusted to 7 with KOH, and 0.2 mL of 1 M $MnSO_4$ and 1.33 mL of 3 M KCL were added to give final concentrations of 1 and 20 mM, respectively. Tartrate dehydrogenase (170 units) and lactate dehydrogenase (50 units) were added, and the solution was incubated at room temperature for 48 h to remove the D-malate-2-*d*. The amount of D-malate-2-*d* remaining in the solution was determined by end-point assay using TDH. The end-point assay contained 100 mM Ches (pH 8.5), 1 mM NAD, 30 mM KCl, 1 mM $MnSO_4$, 50 μg (1 μM) of TDH, and 20 μL of the synthesis reaction solution. After 48 h, more than 95% of the D-malate-2-*d* originally present was removed. After removal of the D-malate-2-*d*, the pH of the solution was adjusted to 5 with perchloric acid and activated charcoal was added to remove the dinucleotides. The solution was filtered and concentrated by rotary evaporation, and the L-malate 2-*d* was purified on a Dowex AG-1-X8 column according to the method of Viola et al. (*17*). The L-malate-2-*d* concentration was determined via an end-point assay containing 100 mM Ches (pH 8.5), 1 mM NAD, 1 mM $MnSO_4$, 5 mM fumarate, 50 μg of wild-type *A. suum* malic enzyme, and ~0.1 mM L-malate-2-*d*.

Enzyme Assays. Enzyme assays were conducted at 25 °C in 1 cm cuvettes using a Beckman DU640 UV−visible

spectrophotometer. In the direction of oxidative decarboxylation of malate, malic enzyme activity was measured at varying concentrations of L-malate, divalent metal ion, NAD, and $(NH_4)_2SO_4$ as indicated in the text. The nonvaried substrate concentration was maintained at a concentration at least 10 times its K_m value. Reaction mixtures were maintained at pH 7 using 100 mM Hepes buffer. The reaction was followed at 340 nm to monitor the production of NADH ($\epsilon_{340} = 6220\ M^{-1}\ cm^{-1}$). Malic enzyme uses the uncomplexed form of the divalent metal ion and substrates (*1*), and corrections for chelate complexes were carried out using the following dissociation constants: 25.1 mM for Mg-malate, 19.7 mM for Mg-NAD, and 19.6 mM for Mg-NADH (*1*, *18*, *19*). All substrate and activator concentrations reported in the text refer to the uncomplexed concentrations of substrates, activators, and metal ions unless noted otherwise. The primary kinetic deuterium isotope effects were determined by direct comparison of initial velocities using 100 mM Hepes (pH 7), 1 mM free NAD, 30 mM free Mg^{2+}, and a varied L-malate-2-*h*(*d*) concentration.

Inhibition Studies. Inhibition patterns were obtained by measuring the initial rate as a function of malate (or NAD) with NAD (or malate) maintained equal to its K_m at different fixed concentrations of oxalate, including zero, K_i, $2K_i$, and $4K_i$. Experiments were carried out in 100 mM Hepes (pH 7) and 30 mM free Mg^{2+}. The inhibition patterns obtained with the malate concentration varied were repeated at several fixed concentrations of NH_4^+. Double-inhibition experiments with NADH and oxalate as inhibitors were also carried out with malate and NAD fixed at their respective K_m values, and via measurement of the initial rate as a function of NADH concentration at different fixed levels of oxalate (0, K_i, $2K_i$, and $4K_i$). Data were plotted in Dixon fashion, $1/v$ versus NADH concentration at different fixed levels of oxalate.

^{13}C Isotope Effects. The technique for the determination of ^{13}C isotope effects was that of O'Leary (*20*) in which the natural abundance of ^{13}C in the C-4 position of L-malate-2-*h*(*d*) was used. Both 100% and low-conversion samples were used, and the $^{12}C/^{13}C$ ratio of the isolated CO_2 from each sample was determined. The relative rates of reaction of ^{12}C versus ^{13}C, and thus the ^{13}C isotope effect, are determined from these ratios. The concentration of L-malate-2-*h*(*d*) was determined by end-point assay prior to preparation of the reaction mixtures. Reaction mixtures for the low-conversion samples contained 25 mM Hepes, 30 mM $MgSO_4$, 12 mM L-malate-2-*h*(*d*), 10 mM NAD, and either 0, 25, or 600 mM NH_4Cl in 33 mL. Full-conversion samples contained 25 mM Hepes, 30 mM $MgSO_4$, 2.2 mM L-malate-2-*h*(*d*), and 10 mM NAD in 33 mL. The reaction mixtures were adjusted to a pH of ~6 and sparged with CO_2 free nitrogen for at least 3 h. The pH was adjusted to pH 8.2 with KOH and the mixture sparged for an additional 2 h. The reactions were carried out in sealed reaction vessels to prevent contamination with atmospheric CO_2. The full conversion sample was initiated by the addition of 0.6 mg of wild-type malic enzyme, and the reaction was allowed to proceed overnight. The full-conversion sample was monitored for completeness of reaction by removing an aliquot of the reaction mixture and checking the absorbance at 340 nm. Concentrated sulfuric acid (100 μL) was added to the reaction mixture prior to isolation of CO_2. The low-conversion samples were initiated by the addition of 0.4−4 mg in 100 μL (depending on NH_4^+ concentration) of the R181Q mutant of malic enzyme. Aliquots were removed at time intervals to check for progress of the reaction, and the reactions were quenched by the addition of 100 μL of concentrated sulfuric acid prior to CO_2 isolation. The isotopic composition of the CO_2 was determined using an isotope ratio mass spectrometer (Finnigan Delta E). All ratios were corrected for ^{17}O according to the method of Craig (*21*).

Data Processing. Initial velocity data were fitted using BASIC versions of the FORTRAN programs developed by Cleland (*22*). Double-inhibition data and data conforming to eqs 7, 10, and 11 were fitted to appropriate equations as discussed below, using the Marquardt−Levenberg algorithm supplied with the EnzFitter program from BIOSOFT (Cambridge, U.K.). Saturation curves were fitted using eq 1. Initial velocity data conforming to an equilibrium ordered or sequential kinetic mechanism were fitted using eqs 2 and 3. Data for competitive, noncompetitive, and double inhibition were fitted to eqs 4−7.

$$v = \frac{V[A]}{K_a + [A]} \tag{1}$$

$$v = \frac{V[AB]}{K_{ia}K_b + K_b[A] + [AB]} \tag{2}$$

$$v = \frac{V[AB]}{K_{ia}K_b + K_a[B] + K_b[A] + [AB]} \tag{3}$$

$$v = \frac{V[A]}{K_a\left(1 + \frac{[I]}{K_{is}}\right) + [A]} \tag{4}$$

$$v = \frac{V[A]}{K_a\left(1 + \frac{[I]}{K_{is}}\right) + [A]\left(1 + \frac{[I]}{K_{ii}}\right)} \tag{5}$$

$$v = \frac{v_o}{1 + \frac{[I]}{K_i} + \frac{[J]}{K_j} + \frac{[IJ]}{\alpha K_i K_j}} \tag{6}$$

$$v = \frac{v_o}{1 + \left(\frac{[\text{oxalate}]}{K_{\text{ioxalate}}}\right)\left(1 + \frac{[\text{NADH}]}{K_{\text{iNADH}}}\right)} \tag{7}$$

In eqs 1−7, v is the initial velocity, v_o is the initial rate in the absence of inhibitors, V is the maximum velocity, K_a and K_b are the Michaelis constants for A and B, respectively, K_{ia} is the dissociation constant for EA, K_{is} and K_{ii} are slope and intercept inhibition constants, respectively, K_i and K_j are inhibition constants for I and J, respectively, in the double-inhibition experiments, and α is the interaction constant, which measures synergy of binding of the two inhibitors. In eq 7, $K_{ioxalate}$ and K_{iNADH} are inhibition constants for oxalate and NADH in the double-inhibition experiments that exhibited no inhibition by NADH in the absence of oxalate.

Data for primary kinetic deuterium isotope effects were fitted using eq 8, where F_i is the fraction of deuterium in the labeled compound and $E_{V/K}$ and E_V are the isotope effects

minus 1 on V/K and V, respectively.

$$v = \frac{V[\mathrm{A}]}{K_a(1 + F_i E_{V/K}) + [\mathrm{A}](1 + F_i E_V)} \quad (8)$$

Calculation of ^{13}C isotope effects made use of eq 9, where f is the fraction of completion of reaction and R_f and R_o are the $^{12}C/^{13}C$ isotopic ratios of CO_2 at partial and complete conversion, respectively.

$$^{13}\left(\frac{V}{K}\right) = \frac{\log(1 - f)}{\log\left[1 - f\left(\frac{R_f}{R_o}\right)\right]} \quad (9)$$

The dependence of the rate constant ($V/K_{malate}E_t$) on the concentration of NH_4^+ adheres to eq 10. Data were not sufficiently conditioned to produce a fit of eq 10 to the data, and the fit was done graphically as discussed in the Results. In eq 10, V_{app1} is the value of the second-order rate constant with NH_4^+ saturating for the first site in R181Q, and K_{NH4} is the activation constant for NH_4^+ for the first site. The second site is difficult to saturate, and V_{app2}/K'_{NH4} is the second-order rate constant for the second phase.

$$\frac{V}{K_{malate}E_t} = \left[\frac{(V_{app})_1}{K_{NH4} + NH_4^+} + \frac{(V_{app})_2}{K'_{NH4}}\right][NH_4^+] \quad (10)$$

Data for the ammonia dependence of $K_{ioxalate}$ and K_{malate} were fitted to eq 11, which describes a hyperbolic function.

$$K = \frac{a\left(1 + \frac{NH_4^+}{K_{num}}\right)}{1 + \frac{NH_4^+}{K_{NH4}}} \quad (11)$$

where K is either $K_{ioxalate}$ or K_{malate}, a is the value of K at zero NH_4^+, K_{num} is a constant that causes the value of K to level off at some finite value at infinite NH_4^+, and K_{NH4} is the activation constant for binding of NH_4^+ to the high-affinity site.

Calculation of Intrinsic Isotope Effects and Commitment Factors. The theory for calculation of intrinsic isotope effects and commitment factors assuming a stepwise mechanism was that of Karsten and Cook (*2*) for malic enzyme. The kinetic mechanism with metal ion and dinucleotide substrate at saturating concentration may be described as in mechanism 12, where M is Mg^{2+}, A is the oxidized dinucleotide, B is L-malate, X is the bound oxaloacetate intermediate, Q is pyruvate, and R is the reduced dinucleotide.

$$\mathrm{EMA} \underset{k_6}{\overset{k_5\mathbf{B}}{\rightleftharpoons}} \mathrm{EMAB} \underset{k_8}{\overset{k_7}{\rightleftharpoons}} \mathrm{E^*MAB} \underset{k_{10}}{\overset{k_9}{\rightleftharpoons}} \mathrm{E^*MXR} \xrightarrow[\mathrm{CO_2}]{k_{11}} \mathrm{E + Q + R} \quad [12]$$

where the rate constants k_5 and k_6 are for malate binding and release, respectively, k_7 and k_8 represent a precatalytic conformational change leading to a complex poised for catalysis, k_9 and k_{10} are for forward and reverse hydride transfer, respectively, and k_{11} represents the decarboxylation step. The affinity of the enzyme for CO_2 is low, and thus, the release of CO_2 is likely fast, making the decarboxylation step irreversible. The equations for the isotope effects are

$$^{D}\left(\frac{V}{K_{malate}}\right) = \frac{^{D}k_9 + c_f + {}^{D}K_{eq}(c_r)}{1 + c_f + c_r} \quad (13)$$

$$^{13}\left(\frac{V}{K_{malate}}\right)_H = \frac{^{13}k_{11} + \frac{1 + c_f}{c_r}}{1 + \frac{1 + c_f}{c_r}} \quad (14)$$

$$^{13}\left(\frac{V}{K_{malate}}\right)_D = \frac{^{13}k_{11} + \frac{1 + c_f/{}^{D}k_9}{{}^{D}K_{eq}(c_r)/{}^{D}k_9}}{1 + \frac{1 + c_f/{}^{D}k_9}{{}^{D}K_{eq}(c_r)/{}^{D}k_9}} = \frac{^{13}k_{11} + \frac{^{D}k_9 + c_f}{{}^{D}K_{eq}(c_r)}}{1 + \frac{^{D}k_9 + c_f}{{}^{D}K_{eq}(c_r)}} \quad (15)$$

The commitment factors, in all cases, are relative to the hydride transfer step. The forward commitment to catalysis, c_f, is $(k_9/k_8)(1 + k_7/k_6)$, and the reverse commitment to catalysis, c_r, is k_{10}/k_{11}. $^{D}k_9$ is the intrinsic primary deuterium kinetic isotope effect; $^{13}k_{11}$ is the intrinsic primary ^{13}C kinetic isotope effect, and $^{D}K_{eq}$ is the deuterium isotope effect on the equilibrium constant [1.18; determined by Cook et al. (*23*)] and is equal to $^{D}k_9/{}^{D}k_{10}$. The commitment factors and intrinsic isotope effects were calculated in a manner similar to that described by Karsten and Cook (*2*) using an iterative method to search for the best fit to the data.

RESULTS

Kinetic Parameters for the R181Q and R181K Mutant Enzymes. Two mutations of the *A. suum* NAD-malic enzyme were made, changing R181 in the binding site for malate to Q and K (Figure 1). Kinetic parameters for each of the mutant enzymes are summarized in Table 1. The most pronounced changes for both of the mutant enzymes are in K_{malate}, which is increased ~100-fold, and in V/E_t, which is decreased nearly 300-fold for R181K and ~20-fold for R181Q, compared to that of the wild-type enzyme. On the other hand, K_{NAD} is increased by a factor of only 2 for R181Q (and unchanged for R181K), and K_{Mg} is increased by 3.7-fold for R181K (and unchanged for R181Q).

Chemical Rescue by NH_4^+. During the course of characterizing the two mutant enzymes, we discovered that R181Q was activated by NH_4^+. In the presence of 60 mM NH_4^+, K_{malate} is reduced to ~8 mM compared to 57 mM in the absence of NH_4^+ and V/E_t is increased ~4-fold, giving a 28-fold increase in $V/K_{malate}E_t$. Guanidinium decreases K_{malate} by only ~2-fold and has no effect on V/E_t. Neither guanidinium nor NH_4^+ has any effect on K_{NAD} or K_{Mg}.

Since there was no or little effect of NH_4^+ on K_{NAD} or K_{Mg}, a detailed analysis of the effect of NH_4^+ concentration on the activity of the R181Q mutant was carried out with the concentration of malate varied at different fixed levels of NH_4^+. Data are shown graphically in panels A and B of Figure 2 with the raw data listed in Table 2. The K_m for malate decreases from 57 mM in the absence of NH_4^+ to a constant value of ~8 mM above 6 mM NH_4^+. [The K_m for NAD is constant over the entire range of NH_4^+ concentrations (data not shown).] On the other hand, V/E_t is constant to ~6 mM and then increases in direct proportion to the

Table 1: Kinetic Parameters of the Wild-Type and R181 Mutant NAD-Malic Enzymes

	wild type[a]	R181K	R181Q	R181Q with 60 mM NH_4^+	R181Q with 60 mM guanidinium
V/E_t (s^{-1})	36 ± 3	0.13 ± 0.01 (277)[b]	2.1 ± 0.2 (17)[b]	7.7 ± 0.8 (4.7)[b]	1.6 ± 0.2 (23)[b]
$V/K_{NAD}E_t$ (M^{-1} s^{-1})	(1.0 ± 0.2) × 10^6	ND[c]	(3 ± 1) × 10^4 (33)[b]	(8 ± 2) × 10^4 (13)[b]	(4.0 ± 0.4) × 10^3 (250)[b]
$V/K_{malate}E_t$ (M^{-1} s^{-1})	(7 ± 1) × 10^4	2.6 ± 0.5 (27000)[b]	37 ± 6 (1900)[b]	963 ± 300 (73)[b]	70 ± 24 (1000)[b]
K_{NAD} (μM)	35 ± 7	ND[c]	70 ± 30 (2)[b]	100 ± 32 (2.9)[b]	120 ± 12 (3.4)[b]
K_{malate} (mM)	0.53 ± 0.07	50 ± 10 (94)[b]	57 ± 13 (108)[b]	8 ± 1 (15)[b]	23 ± 8 (43)[b]
K_{Mg} (mM)	4.5 ± 1.7	16 ± 4 (3.7)[b]	5 ± 2 (1.1)[b]	7 ± 2 (1.6)[b]	ND[c]

[a] Data from ref *15*. [b] Values in parentheses are the *x*-fold decrease in V/E_t and V/KE_t or the *x*-fold increase in K_m compared to those of the wild type. [c] Not determined.

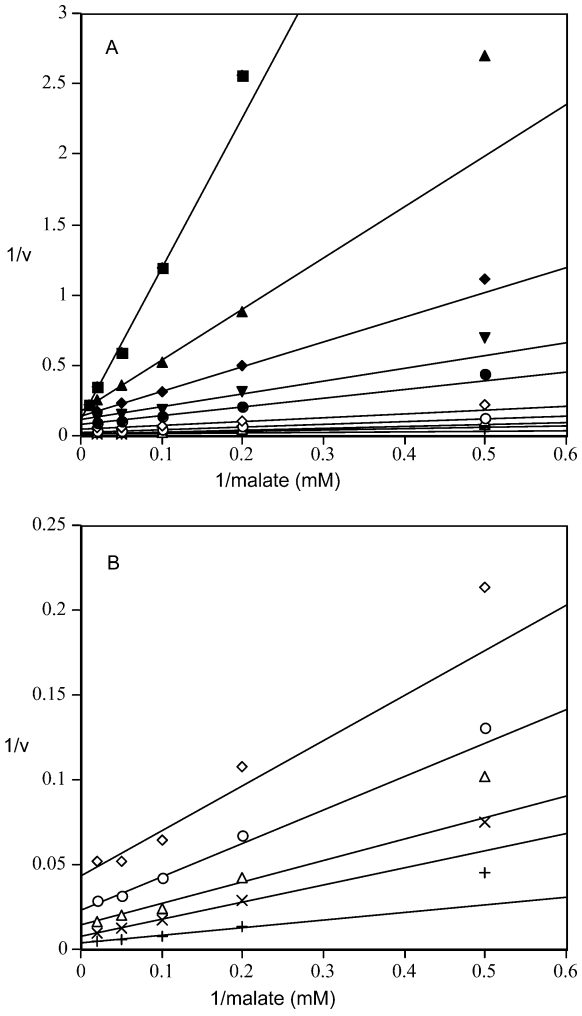

FIGURE 2: Dependence of the initial velocity on the concentrations of malate and NH_4^+. The Mg^{2+} and NAD concentrations were maintained at 10 times their K_d and K_m values, respectively, and malate was varied. The data points are the experimentally determined initial rates (μM per minute), and the lines are from a fit of the data to eq 1 at each of the fixed NH_4^+ concentrations. (A) Data for all NH_4^+ concentrations are shown: 0 (■), 1.5 (▲), 4 (◆), 6 (▼), 10 (●), 25 (◇), 60 (○), 120 (△), 300 (×), and 600 mM (+). (B) Only NH_4^+ concentrations of ≤25 mM are shown using the same symbols as in panel A.

concentration of NH_4^+. Plots of V/E_t and $V/K_{malate}E_t$ versus the concentration of NH_4^+ are clearly biphasic (Figure 3A,B). The first- and second-order rate constants (V/E_t and $V/K_{malate}E_t$, respectively) reflect predominantly specific forms of enzyme and substrate; $V/K_{malate}E_t$ reflects free malate and the E−NAD−Mg−NH_4^+ complex, while V/E_t reflects the E−NAD−Mg−NH_4^+−malate complex. The biphasic nature of the $V/K_{malate}E_t$ plot indicates that two binding sites exist on the enzyme for NH_4^+, likely reflecting the A and B nitrogen sites of the guanidinium moiety vacated upon mutation of R to Q (Figure 1A). If correct, binding of the second molecule of ammonia is likely as the neutral species given the charge repulsion expected if both were positively charged. As suggested in Data Processing, data likely adhere to eq 10, which describes the sum of two saturation curves. Although the data can be fitted to eq 10, standard errors are large, suggesting the data are not well-conditioned. However, an estimate of K_{NH4}, the activation constant for binding to the first of the two sites, can be obtained from a fit of K_{malate} versus NH_4^+, and this gives a value of 0.7 ± 0.1 mM (Figure 4); on the other hand, V_{app1}, the value of $V/K_{malate}E_t$ at saturating NH_4^+ for the first site, is obtained by extrapolating the linear portion of Figure 3A (observed above 25 mM NH_4^+) to zero, giving a value of ~500 M^{-1} s^{-1}. The value of $V_{app2}/K'_{NH4}E_t$ is estimated as the slope of the linear portion of the curve in Figure 3A, ~3700 M^{-2} s^{-1} (this is a third-order rate constant that is first order in enzyme, malate, and NH_4^+).

Interestingly, the maximum observed value of V/E_t at 600 mM NH_4^+ is 34 s^{-1}, identical within error to the value of 36 s^{-1} obtained for the wild-type enzyme. From a plot of V/E_t versus NH_4^+ (data not shown), estimates of K'_{NH4}, the activation constant for ammonia binding to the second site, and the maximum V/E_t at saturating ammonia are 420 ± 90 mM and 45 ± 7 s^{-1}, respectively, at pH 6.5.

The effect of $(NH_4)_2SO_4$ on wild-type enzyme activity was investigated and found to have no activating effect up to 600 mM. Some weak inhibition, presumably by SO_4^{2-}, was detected at concentrations of ≥300 mM.

Oxalate Inhibition. Oxalate is the tightest binding inhibitor known for the NAD-malic enzyme (K_i = 6 μM) and is an analogue of the enolpyruvate intermediate produced upon decarboxylation of oxaloacetate (*24*). At all NH_4^+ concentrations investigated, oxalate is a competitive inhibitor versus malate at saturating NAD. The K_i value is highest at very low NH_4^+ concentrations and decreases as the NH_4^+ concentration increases (Figure 4). The dependence of $K_{ioxalate}$ on NH_4^+ gives an activation constant of ~0.7 ± 0.1 mM, similar to that obtained from the dependence of K_{malate} on NH_4^+. In the presence of 10 mM NH_4^+, oxalate is a noncompetitive inhibitor versus NAD with malate fixed near its K_m value. Data are summarized in Table 3.

A double-inhibition pattern varying oxalate and NADH in the presence of 10 mM NH_4^+ is shown in Figure 5. In the absence of oxalate, NADH, a product of the reaction, inhibits the enzyme as shown by the increase in the intercept in Figure 5 as the NADH concentration increases from 0 to 100 μM. Inhibition by oxalate in the absence of NADH is

Table 2: Effect of NH_4^+ on the Kinetic Parameters of the R181Q Mutant of NAD-Malic Enzyme

$[NH_4^+]$ (mM)	V/E_t (s^{-1})[a]	$V/K_{NAD}E_t$ (M^{-1} s^{-1})	$V/K_{malate}E_t$ (M^{-1} s^{-1})	K_{NAD} (μM)	K_{malate} (mM)
0	1.6 ± 0.1	(2.3 ± 0.8) × 10^4	28 ± 5	70 ± 30	57 ± 13
1.5	1.5 ± 0.2	(1.0 ± 0.3) × 10^4	46 ± 11	99 ± 35	21 ± 2
4	1.7 ± 0.2	(7.5 ± 1.2) × 10^3	94 ± 10	160 ± 40	12 ± 1
6	1.7 ± 0.2	(1.4 ± 0.3) × 10^4	183 ± 24	110 ± 32	8 ± 2
10	1.9 ± 0.2	(2.9 ± 0.6) × 10^4	276 ± 88	72 ± 20	8 ± 1
25	3.3 ± 0.3	(4.8 ± 1.2) × 10^4	634 ± 343	81 ± 27	6 ± 2
60	5.8 ± 0.6	(6.4 ± 1.4) × 10^4	777 ± 247	100 ± 42	8 ± 1
120	10.5 ± 0.8	(1.1 ± 0.3) × 10^5	1192 ± 212	99 ± 42	8 ± 2
300	19 ± 1	(1.9 ± 1.4) × 10^5	1504 ± 77	100 ± 76	13 ± 1
600	34 ± 3	ND[b]	3400 ± 570	ND[b]	10 ± 3

[a] For comparison, the wild-type parameters are given in column 1 of Table 1. [b] Not determined.

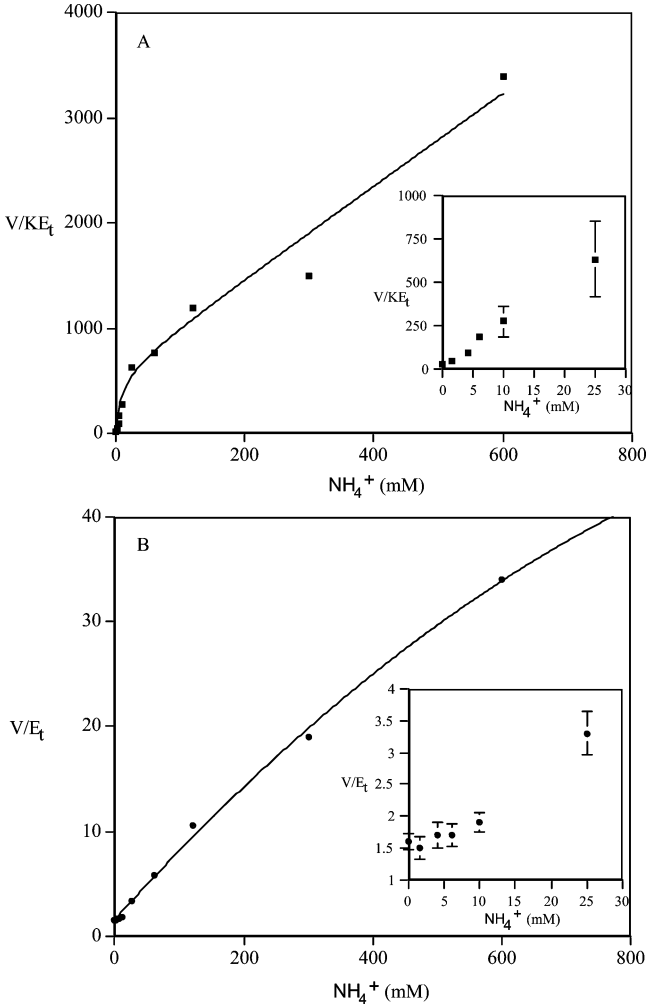

FIGURE 3: Dependence of $V/K_{malate}E_t$ and V/E_t on NH_4^+ obtained from the data in Figure 2. The curves are drawn by eye.

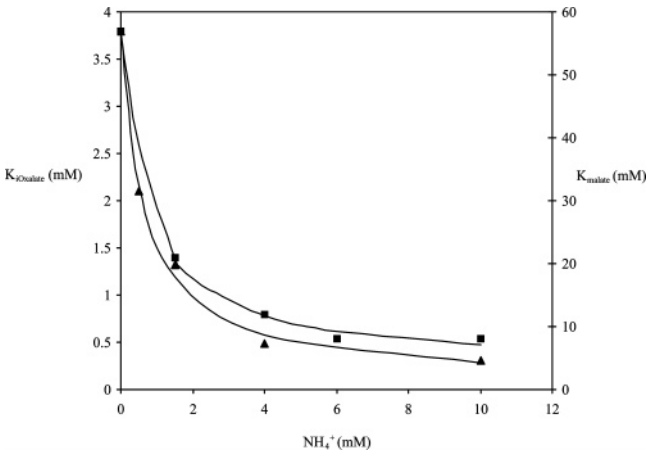

FIGURE 4: Dependence of K_{malate} (■) and $K_{ioxalate}$ (▲) on the concentration of NH_4^+. The data points are the experimentally determined values, and the lines are derived from a fit of the data using eq 11. The $K_{ioxalate}$ was determined at each NH_4^+ concentration from an inhibition pattern with malate varied, NAD fixed at 1 mM, and Mg^{2+} fixed at 30 mM (pH 6.5). Values were estimated from a fit using eq 4. The K_{malate} values are from Table 2. Estimated values of parameters in eq 11 are as follows for K_{malate}: $a = 57 \pm 1$, $K_{num} = 12 \pm 6$, and $K_{NH4} = 0.72 \pm 0.11$. They are as follows for $K_{ioxalate}$: $a = 3.8 \pm 0.1$, $K_{num} = 43 \pm 106$, and $K_{NH4} = 0.65 \pm 0.11$.

Table 3: Dead-End Inhibition by Oxalate of the R181Q Mutant Enzyme as a Function of NH_4^+ Concentration[a]

varied substrate	fixed substrate	$[NH_4^+]$ (mM)	inhibition pattern[b]	K_{is} ± SE (mM)	K_{ii} ± SE (mM)
malate	NAD (1 mM)	0.5	C	1.8 ± 0.2	
malate	NAD (1 mM)	10	C	0.38 ± 0.07	
malate	NAD (1 mM)	600	C	0.17 ± 0.03	
NAD	malate (10 mM)	10	NC	0.27 ± 0.06	0.7 ± 0.2

[a] Data were obtained at pH 6.5 with 30 mM Mg^{2+}. [b] C and NC are competitive and noncompetitive, respectively.

also evident. Oxalate and NADH inhibition are synergistic as shown by the increase in the slope in Figure 5 as the NADH concentration increases from 0 to 100 μM. A fit of the data to eq 6 gives values of K_{iNADH}, $K_{ioxalate}$, and α of 170 ± 10 μM, 472 ± 20 μM, and 0.220 ± 0.025, respectively. In the absence of NH_4^+ and in the presence of 600 mM NH_4^+ (data not shown), no inhibition by NADH is observed up to 0.2 mM in the absence of oxalate, but even greater synergistic binding is observed; the K_{iNADH} is decreased to 68 ± 18 μM in the absence of NH_4^+ and to 16 ± 2 μM in the presence of 600 mM NH_4^+ in the presence of oxalate (Table 4).

Isotope Effects. To further investigate the role of R181 in binding and catalysis, primary deuterium and ^{13}C isotope effects were determined for the R181Q mutant of malic enzyme in the absence and presence of different NH_4^+ concentrations. Data are summarized in Table 5. Values of $^D(V/K)$ are relatively small and similar to those obtained for the wild-type enzyme. As an internal check of the data, values for $^D(V/K)$ were calculated from the measured values of the ^{13}C isotope effects and $^DK_{eq}$ (Table 5) and are similar to the experimentally determined values in all cases. Values of ^DV are larger than $^D(V/K)$ and similar to those of the wild-type enzyme in the absence and presence of NH_4^+. In contrast to the deuterium isotope effects, the ^{13}C isotope effects are

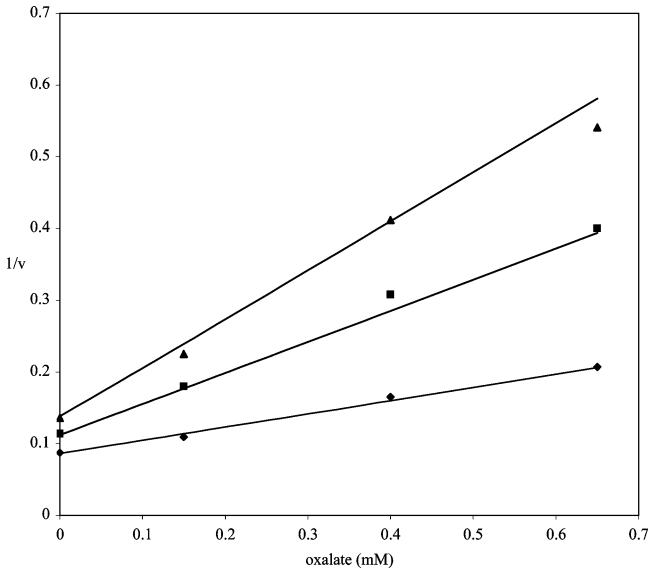

FIGURE 5: Double inhibition of R181Q by oxalate and NADH at pH 6.5 and 10 mM NH_4^+. The NADH concentrations are 0 (▲), 0.05 (■), and 0.1 mM (◆). The concentrations of Mg^{2+}, malate, and NAD were 30, 10, and 0.1 mM, respectively. The data points shown are the experimentally determined values, and the lines are derived from a fit of the data to eq 6.

Table 4: Kinetic Parameters from Oxalate/NADH Double Inhibition for the R181Q Mutant[a]

$[NH_4^+]$ (mM)	$K_{iNADH} \pm$ SE (μM)	$K_{iNADH} \pm$ SE (μM) with oxalate	$K_{ioxalate} \pm$ SE (μM)	$\alpha \pm$ SE
0	UD[b]	68 ± 18	1520 ± 170	
10	170 ± 10		472 ± 20	0.217 ± 0.025
600	UD[b]	16 ± 2	238 ± 16	
wt	100 ± 20		13 ± 1	0.054 ± 0.015

[a] Data for the wild type and 10 mM NH_4^+ were fitted using eq 6, and data for 0 and 600 mM NH_4^+ were fitted using eq 7. [b] Undefined.

considerably larger than the values measured for the wild-type enzyme. The largest ^{13}C isotope effect is observed in the absence of NH_4^+ (1.0486) and is smaller (1.0417) in the presence of low and high NH_4^+ concentrations. In all cases, $^{13}(V/K)_H$ is significantly greater than $^{13}(V/K)_D$ and data adhere, within error, to the equality given in footnote b of Table 5, consistent with the stepwise oxidative decarboxylation proposed for the wild-type enzyme (*2*−*4*).

DISCUSSION

R181 Mutant Enzymes. A change in the arginine, R181, in the reactant-binding site to Q and K results in an enzyme that has significant changes in kinetic parameters. As shown in Table 1, V/E_t is decreased nearly 300-fold in the case of R181K and ~20-fold for R181Q, suggesting the residue is important, but not essential to the enzyme's catalytic function. Since the change to K affects V/E_t more than the change to the smaller Q, the longer side chain impairs function even though it has a positive charge, as does R. This is likely because the equivalent of only one of the nitrogen functional groups of the guanidinium side chain is present, and this may lead to improper positioning of malate with respect to NAD, an improper conformation of the active site, or both.

In addition to the effect on V/E_t, there is a significant increase in K_{malate} and $K_{ioxalate}$. The K_m for malate increases by ~100-fold for the two mutant enzymes, while changes in K_{NAD} are negligible (2-fold increase for R181Q) and K_{Mg} (3.7-fold increase for R181K and no change for R181Q). In the wild-type enzyme, K_{malate} and K_{NAD} are equal to their respective K_d values for release of malate or NAD from the E−NAD−Mg−malate complex (*24*), and thus, R181 is responsible for ~2.6 kcal/mol in malate binding energy $\{\Delta\Delta G^{\circ\prime} = RT \ln[(K_{malate})_{R181Q}/(K_{malate})_{wt}]\}$ but provides essentially no affinity for NAD. This is not a surprising result given the direct hydrogen bonding interaction between R181 and the α-carboxylate of malate. Consistent with these data are the inhibition studies carried out with oxalate. Oxalate is a competitive inhibitor versus malate, an analogue of enolpyruvate, and the tightest binding inhibitor known for malic enzyme (*24*, *25*). For the wild-type enzyme at pH 6.5, oxalate is a noncompetitive inhibitor versus malate at saturating NAD with a K_{is} of 50 μM and a K_{ii} of 290 μM (*24*). The K_{is} results from oxalate binding to E-NAD, competing with malate, while K_{ii} was proposed to result from binding of oxalate to an unisomerized E−NAD complex (*26*). In contrast, oxalate is a strict competitive inhibitor versus malate at pH 6.5 for the R181Q mutant enzyme with a K_i of 1.8 mM, a 36-fold increase in the K_{is} value compared to that of the wild type. The change in affinity is similar to that observed for malate, consistent with oxalate mimicking the enolpyruvate intermediate and accepting a hydrogen bond from R181. The 3-fold difference in the loss of affinity for oxalate compared to malate is almost certainly a result of the interaction of the two negatively charged carboxylates of oxalate with the divalent metal ion. The inhibition by oxalate does not exhibit the intercept effect observed for the wild-type enzyme (noncompetitive inhibition). If the ratio of the affinities for the two forms of the E−NAD complex is maintained for the R181Q mutant enzyme, a K_{ii} value of >10 mM would be expected, and this is outside the concentration range used in these studies.

Finally, the R181 side chain provides binding affinity for NADH. Inhibition by NADH in the absence of NH_4^+ and oxalate is not detected up to 0.2 mM, more than 10-fold greater than the inhibition constant for the wild-type enzyme (*24*). Thus, K_{iNADH} for R181Q is increased by at least 1 order of magnitude compared to that of the wild-type enzyme. As discussed in the introductory section, the three-dimensional structures of bound oxidized and reduced dinucleotide substrates differ in the position of the nicotinamide ring with that for the reduced nicotinamide rotated by more than 180° compared to that of the oxidized substrate such that it impinges on the L-malate binding site (*8*, *9*). One can rationalize the importance of the rotation in terms of the proper positioning of the oxaloacetate intermediate for decarboxylation once it has been displaced by the nicotinamide ring. However, there was a question of whether this rotation of the ring is on the reaction pathway. 6-Phosphogluconate dehydrogenase exhibited a similar ring rotation on the basis of structures, and its import in the catalytic pathway was corroborated using site-directed mutagenesis of residues that interact with the nicotinamide ring of NADP, but not NADPH. The mutant enzymes all gave a 1 order of magnitude increase in the K_{iNAD} with no change in K_{iNADH}. Given the results obtained in these studies, the >10-fold increase in K_{iNADH} with little change in K_{iNAD} is consistent with the rotation of the nicotinamide ring of NAD as it is

Table 5: Isotope Effects for the R181Q NAD-Malic Enzyme as a Function of NH_4^+

$[NH_4^+]$ (mM)	$^D(V/K_{malate})^a$	$^D(V/K_{malate})_{calc}{}^b$	^DV	$^{13}(V/K_{malate})_H$	$^{13}(V/K_{malate})_D$
0	1.39 ± 0.06	1.49	1.9 ± 0.1	1.0486 ± 0.0023	1.0384 ± 0.0006
25	1.57 ± 0.16	1.59	2.9 ± 0.4	1.0417 ± 0.0022	1.0309 ± 0.0007
600	1.65 ± 0.08	1.57	2.0 ± 0.1	1.0418 ± 0.0006	1.0314 ± 0.0003
wild type[c]	1.57	1.60	2.0	1.0342	1.0252

[a] Values are averages from at least three separate determinations for all of the isotope effects. [b] Calculated from $^D(V/K_{malate})/^DK_{eq} = {}^{13}(V/K_{malate})_H - 1/{}^{13}(V/K_{malate})_D - 1$, where $^DK_{eq}$ equals 1.18 (*23*). [c] Values are from refs *2* and *3*.

Table 6: Intrinsic Isotope Effects and Commitment Factors Estimated from the Data in Table 5

$[NH_4^+]$ (mM)	c_f	c_r	$^{13}k_{11}$	$^Dk_9$
0	0.10 ± 0.04	9.1 ± 0.4	1.0544 ± 0.0005	4.4 ± 0.1
25	1.0 ± 0.6	8.9 ± 0.7	1.0513 ± 0.0024	5.9 ± 0.5
600	1.0 ± 0.5	9.5 ± 1.3	1.0506 ± 0.0019	5.9 ± 0.6
wild type[a]	6.6	14.3	1.052	10.8

[a] Values are from ref *2*.

reduced to NADH, causing the oxaloacetate intermediate to reposition so that decarboxylation is facilitated. This mechanical catalysis may be a mode common to the pyridine nucleotide-linked β-hydroxy acid oxidative decarboxylases. The stereochemistry of the hydride transfer reaction is specific with transfer of the hydride to the *re* face of the nicotinamide ring. Thus, equilibrium must exist between the two conformations of the nicotinamide ring, that is, that for NAD and that for NADH. The equilibrium is likely random given the low kinetic barrier to rotation. However, binding of the nicotinamide ring must be favored in one position or the other depending on whether the ring is oxidized or reduced.

The decrease in the rate of the reaction must result from a decrease in the rates of several steps along the reaction pathway. The deuterium and ^{13}C isotope effects are informative in this respect. The magnitude of the deuterium isotope effect was not altered to any extent in the R181Q mutant enzyme; $^D(V/K_{malate})$ is ~1.6 for the wild-type enzyme and 1.4 for R181Q. However, $^{13}(V/K_{malate})_H$ is increased from 1.035 to 1.049, which is close to the intrinsic isotope effect of 1.052, suggesting the decarboxylation step almost completely limits the overall reaction (Table 6). This may result from the inability of Q in the R181Q mutant enzyme to properly position the oxaloacetate intermediate and the reduced cofactor with respect to the protein matrix, consistent with the role of the nicotinamide ring and R181 in catalysis (see above).

Rescue of R181Q Activity by NH_4^+. During the course of characterizing the mutant enzymes, we discovered that much of the enzyme activity of the R181Q mutant enzyme could be rescued by guanidinium or ammonium ion; ammonium ion was much more effective in rescuing activity than guanidinium. Binding of NH_4^+ to the R181Q mutant enzyme is reasonable since the shorter glutamine residue would leave a pocket where the guanidinium group of arginine was located in the wild-type enzyme (Figure 1A). Since a low NH_4^+ ion concentration decreases K_{malate} by ~8-fold compared to the value in its absence, NH_4^+ must bind in a way that allows interaction with the α-carboxylate of malate.

The biphasic nature of the $V/K_{malate}E_t$ activation indicates combination of 2 mol of NH_4^+ per mole of enzyme active site. The first of the two sites has relatively high affinity at pH 7 and exhibits saturation with an apparent K_{NH4} of ~0.7 mM determined from the change in K_{malate} (Figure 4). Since occupation of the high-affinity site for NH_4^+ results only in a change in K_{malate}, an interaction is likely made with the α-carboxylate of malate, suggesting the first NH_4^+ occupies the position of the A nitrogen of the absent guanidinium group of R181 (Figure 1A). The activation, as a result of occupying this site, is ~8-fold on K_{malate} with no change in V/E_t. Compared to that of the wild-type enzyme, $V/K_{malate}E_t$ is reduced ~2000-fold in the R181Q mutant enzyme and is still ~140-fold lower when the high-affinity NH_4^+ site is occupied. In contrast, V/E_t is reduced ~20-fold whether or not NH_4^+ occupies the high-affinity site; once all reactants and NH_4^+ are bound, the enzyme is reasonably efficient given the 5% remaining activity. Since V/K_{malate} includes the steps for malate binding, while V does not, the difference in activation reflected by the two rate constants is a reflection of the decrease in affinity for malate, likely an increase in the off-rate constant for malate from the E−NAD−Mg−malate complex; data are consistent with the 100-fold increase in K_{malate}.

At higher NH_4^+ concentrations, where the second molecule of activator binds, V/E_t and $V/K_{malate}E_t$ increase together in a 1:1 ratio, and K_{malate} does not change. The process does not saturate up to 600 mM NH_4^+, indicating a much lower affinity for the second molecule of activator. The lower affinity suggests a number of possibilities. One possibility, however, is that the two molecules of NH_4^+ bind at adjacent positions occupying the positions vacated by the guanidinium nitrogens of R181. It is likely that the first molecule binds as NH_4^+ in position A (Figure 1A), given the increase in the affinity of the NH_4^+−E−NAD−Mg complex for malate. Given the charge on the first molecule and consistent with the two molecules mimicking the guanidinium nitrogens of R181, the second molecule likely binds as the neutral species in position B (Figure 1A). The specific sites where NH_4^+ and NH_3 bind and the associated protonation states are currently under investigation. The pK_a for NH_4^+ is 9.3 (*18*), and data were obtained at pH 7. As a result, the concentration of NH_3 present is 0.56% of the added NH_4^+ concentration, so 10−600 mM NH_4^+ gives a NH_3 concentration of 0.056−3.4 mM. Interestingly, V/E_t increases to become equal to the value of the wild-type enzyme at 600 mM NH_4^+, and a double-reciprocal plot of V/E_t versus NH_4^+ (Figure 3) gives an estimate of 45 s^{-1} for the maximum value of V/E_t, ~1.25 times the value of the wild-type enzyme activity. The affinity of R181Q for malate does not increase at the higher NH_4^+ concentrations, suggesting the second activator molecule functions only to increase the rate(s) of steps that limit the overall reaction. This aspect will be considered in detail below in Interpretation of Kinetic Isotope Effects.

Although oxalate is noncompetitive versus malate for the wild-type enzyme at pH 6.5, it is a competitive inhibitor versus malate for R181Q at all NH_4^+ concentrations that were tested. The intercept effect reflects binding of oxalate to the nonisomerized form of the E−NAD complex (*26*). As discussed above, the absence of the intercept effect with malate as the varied reactant is consistent with the explanation suggested for oxalate binding in the absence of NH_4^+; i.e., the nonisomerized form of the enzyme has a very low affinity for oxalate with R181Q. In general, $K_{ioxalate}$ values for R181Q follow the same trend observed for K_{malate}, relatively weak binding in the absence of NH_4^+ ($K_i = 2-4$ mM) and stronger binding in the presence NH_4^+ ($K_i = 0.2-0.4$ mM), consistent with the effect of NH_4^+ on malate and oxalate binding.

Double-inhibition experiments with oxalate and NADH indicate synergistic binding in R181Q similar to that observed for the wild-type enzyme (*24*). K_{iNADH} is decreased from a value that is ≥2 mM in the absence of NH_4^+ to 170 μM in the presence of low concentrations of NH_4^+, consistent with the proposed role of NH_4^+ as a mimic of one of the nitrogens of the guanidinium side chain of R181, i.e., interaction with the nicotinamide carboxamide of NADH giving an increase in affinity for the reduced cofactor. Note that NH_4^+ is not a perfect mimic since K_{iNADH} and $K_{ioxalate}$ do not become equal to values estimated for the wild-type enzyme (Table 4).

In the absence of NH_4^+ or in the presence of 600 mM NH_4^+, there is no significant affinity of the R181Q mutant enzyme for NADH. However, addition of oxalate increases the affinity of NADH substantially. In the absence of NH_4^+, the presence of oxalate leads to a significant decrease in K_{iNADH}, indicating that the synergistic effect of oxalate binding on NADH affinity occurs in the absence of NH_4^+. In the absence of oxalate, a high NH_4^+ concentration leads to an increase in K_{iNADH}, suggesting the second activator that binds interferes with the interaction of the nicotinamide carboxamide with bound NH_4^+. However, with oxalate present, the lowest K_{iNADH} is observed and suggests that either the NH_4^+−carboxamide interaction is restored in the complex with oxalate or the enzyme can adopt a more closed conformation that facilitates NADH binding. Assuming the two NH_4^+ or NH_3 molecules bound to enzyme reside in the guanidinium nitrogen-binding sites vacated in the R181Q mutant enzyme, the situation would be the closest mimic of the wild-type enzyme with an intact R181. Occupancy of both sites may allow the active site to close and could account for the increased affinity for NADH. In the wild-type enzyme, the NADH−enolpyruvate complex, mimicked by the NADH−oxalate complex, is in a closed conformation.

Interpretation of Kinetic Isotope Effects. As indicated above, a $^{13}(V/K_{malate})_H$ value of 1.049, close to the intrinsic isotope effect of 1.052, suggested nearly rate-determining decarboxylation for R181Q in the absence of NH_4^+. This was thought to be a result of improper positioning of the oxaloacetate intermediate and the reduced cofactor. The value of ^DV is invariant (with the possible exception of that measured in the presence of 25 mM NH_4^+, which has a larger standard error) and similar to that measured for the wild-type enzyme. At face value, data suggest that the step(s) that limits the wild-type reaction at saturating substrate concentrations still limits for R181Q in the absence or presence of NH_4^+; i.e., although the rate has decreased, the relative rates of steps at saturating substrate concentrations are the same. In the presence of 25 or 600 mM NH_4^+, the primary deuterium isotope effect on V/K increases slightly to become equal to that of the wild-type enzyme, while $^{13}(V/K_{malate})_H$ decreases slightly from 1.0486 to 1.0417. Values of $^D(V/K)$ can also be calculated from the ^{13}C isotope effects and $^DK_{eq}$ (Table 5 footnote) and provide an accurate estimate because of the accuracy of the ^{13}C isotope effects. There is good agreement between the experimentally determined values and the calculated values for $^D(V/K)$ (Table 5). The increase in $^D(V/K)$ in the presence compared to the absence of NH_4^+ indicates a slight increase in the rate of limitation of the hydride transfer step. However, the deuterium isotope effect cannot be considered as an isolated effect and must be interpreted in conjunction with the ^{13}C isotope effects.

In contrast to the deuterium isotope effects, which are generally similar to those of the wild-type enzyme, the ^{13}C isotope effects are in all cases significantly larger than the wild-type values. The larger $^{13}(V/K)_H$ values, with and without NH_4^+, suggest that decarboxylation is almost completely rate-limiting for R181Q in the absence or presence of NH_4^+. There is a slight but significant decrease in $^{13}(V/K)_H$ in the presence of NH_4^+ concomitant with the slight increase in the value of $^D(V/K)$. To interpret the isotope effect data, estimates of the commitment factors and intrinsic isotope effects were calculated as discussed in Materials and Methods and are presented in Table 6.

The calculated values suggest changes in two parameters for R181Q compared to the wild-type enzyme. The first is in the forward commitment to catalysis, $(k_9/k_8)(1 + k_7/k_6)$. In the absence of NH_4^+, c_f decreases by >60-fold compared to the that of the wild-type enzyme. In the presence of NH_4^+, c_f increases by a factor of 10 from ∼0.1 to ∼1 compared to the value of 6.6 for the wild-type enzyme. The forward commitment can be separated into an internal component ($c_{fint} = k_9/k_8$) and an external component [$c_{fext} = (k_9/k_8)(k_7/k_6)$]. The large increase in K_{malate} (100-fold) can, as stated above, be attributed to an increase in the off-rate constant for malate. Thus, for the wild-type enzyme, the overall commitment of 6.6 is dominated by the internal component; i.e., the rate constant for opening the site to release reactant is slower than the rate of forward hydride transfer ($k_8 < k_9$) by a factor of ∼6. A very small c_f for R181Q in the absence of NH_4^+ implies the essential loss of the internal component of c_f and suggests $k_8 \gg k_9$. An alternative possibility is that with R181Q in the absence of NH_4^+ the site does not fully close and catalysis proceeds from a relatively open conformation of the E−Mg−NAD−malate complex. Incomplete closure of the site may be reasonable since R181 appears to link together NAD, malate, and the protein via L183. The presence of NH_4^+ leads to an increase in the forward commitment that is likely a reflection of a decrease in k_8 and suggests that bound NH_4^+ may promote some closure of the site or the interaction between the bound NH_4^+ and malate may slow release of malate.

The other significant change resulting from the mutation is in the value of the intrinsic deuterium isotope effect, $^Dk_9$. If the only change in relative rate constants is for the precatalytic conformational change for R181Q, then a decrease in the forward commitment for hydride transfer would lead to an increase in $^D(V/K)$. For example, setting $^Dk_9$, $^{13}k_{11}$, and c_r to the wild-type values of 10.8, 1.052, and

14.3, respectively, and assuming $c_f = 0.1$, the calculated values for the V/K isotope effects are as follows: $^{D}(V/K) = 1.8$, $^{13}(V/K)_H = 1.0483$, and $^{13}(V/K)_D = 1.0316$. The calculated deuterium effect is larger than the experimental value, and the ^{13}C isotope effects do not match the experimentally determined values. For R181Q, $^{D}(V/K)$ decreases compared to that of the wild-type enzyme, and considering the decrease in c_f, this suggests the intrinsic deuterium effect must decrease. There are two lines of evidence suggesting that there is a significant tunneling correction in the hydride transfer step for the wild-type enzyme, the estimated value of $^{D}k_9$ (*2*, *4*), and measured α-secondary deuterium kinetic isotope effects that are larger than $^{\alpha-D}K_{eq}$ (*6*). In addition, Klinman[2] has recently suggested that hydrogen isotope effects result from quantum mechanical tunneling and are correlated with breathing modes of the protein, resulting in "gating" with tunneling occurring when the reaction coordinate is shortened. Tunneling would thus be favored in a case where closure of the active site leads to compression of the transition state. A decrease in $^{D}k_9$ from 10.8 in the wild type to ~4.5 for R181Q would be consistent with a loss of hydrogen tunneling for R181Q and perhaps a more open active site, and/or a lengthening of the reaction coordinate. Removing the guanidinium side chain of R181 in the R181Q mutant enzyme would create a "hole" in the active site and also, in accord with the above discussion, potentially lead to an impaired ability of R181Q to fully close the active site given the potential role of R181 in linking together malate, NADH, and the protein via a hydrogen bond to L183. In addition, the loss of the interaction between R181 and the α-carboxylate of malate may lead to misalignment of malate in the active site, and this could have an additional effect on the hydride transfer step. Addition of NH_4^+ leads to an increase in the calculated value of $^{D}k_9$ that, given the decrease in K_{malate}, likely means NH_4^+ binds in the pocket vacated by the guanidinium group of R181 and is thus in position to interact with the α-carboxylate of malate and enhance binding of malate. Therefore, malate would be expected to be oriented differently than in the absence of NH_4^+ and could lead to the observed increase in $^{D}k_9$, which could lead to a restoration of tunneling.

The calculated intrinsic ^{13}C isotope effect in the absence and presence of NH_4^+ varies from about 5.1 to 5.4% with an average value of 5.2%, identical to that calculated for the wild-type enzyme. Data suggest that R181 has little or no effect on the transition state for decarboxylation. The nonenzymatic ^{13}C isotope effect for the metal-catalyzed decarboxylation of oxaloacetate is ~4.9% (*5*), and the intrinsic isotope effect for the chicken liver NADP malic enzyme with Mg^{2+} as the metal ion was determined to be 4.9% (*27*). It appears that in all cases it is the Mg^{2+} ion acting as a Lewis acid that is primarily responsible for determining the transition state structure for decarboxylation. The large intrinsic ^{13}C isotope effect suggests a late transition state for decarboxylation that is not affected by the R181Q mutation. The ^{13}C isotope effect is expressed to a larger extent on $^{13}(V/K)$ in the R181Q mutant than for wild-type enzyme even though the intrinsic value appears not to have changed. The forward internal commitment for decarboxylation is $k_{11}/k_{10}(1 + k_9/k_8)$. The full forward commitment would contain the term k_7/k_6 but is likely near zero for both the wild type and the R181Q mutant as indicated above. Also, as indicated above, for the R181Q mutant in the absence of NH_4^+, k_8 is very fast, and consequently, the forward commitment for decarboxylation reduces to k_{11}/k_{10}, which will be small. Thus, the increase in $^{13}(V/K)$ with the R181Q mutant compared to the wild type is due in large part to the large decrease in k_9/k_8, the internal forward commitment of the hydride transfer step.

The NH_4^+ Effect Is Consistent with the Concerted Model for Allosteric Activation. The primary deuterium isotope effects, $^{D}(V/K)$ and ^{D}V, and the ^{13}C isotope effects change as the NH_4^+ concentration increases to 25 mM. The observed deuterium isotope effect increases from 1.4 to 1.6, while the ^{13}C isotope effect decreases from 4.9 to 4.2%. The change likely reflects, in addition to the 10-fold increase in c_f, a change in the partition ratio of the oxaloacetate intermediate (k_{10}/k_{11}) to favor decarboxylation. The calculated value of c_r is within error identical at all ammonia concentrations (Table 6), which argues against a change in c_r. However, if only c_f increases as indicated in the table, both $^{D}(V/K)$ and $^{13}(V/K)$ would be expected to decrease. The increase in $^{D}(V/K)$ and concomitant decrease in $^{13}(V/K)$ are consistent with the proposed change in c_r; the change is consistent with the proposed role of R181 in facilitating decarboxylation by stabilizing the reduced nicotinamide ring of NADH once it has rotated into the malate binding site.

A further increase in NH_4^+ concentration from 25 to 600 mM does not affect the isotope effects. This is true in spite of the fact that V/E_t increases substantially (20-fold) over this concentration range. These data suggest an equilibrium exists between a less active and more active form of the R181Q mutant enzyme, and in the absence of NH_4^+ (or at low NH_4^+ concentrations), the equilibrium lies greatly in favor of the less active form. As NH_4^+ increases such that the second site is occupied, the equilibrium between the active and less active forms is shifted in favor of the active form leading to the increase in V/E_t.

Data for the R181Q mutant enzyme are thus consistent with the Monod model (*28*). The value of L, the equilibrium constant for the R to T interconversion, can be estimated from the value of V/E_t. In the absence of NH_4^+, V/E_t is 1.6 s^{-1}, ~1/20 of the value of the wild-type enzyme. Assuming the wild-type enzyme value reflects 100% active enzyme, a reasonable assumption since V/E_t reaches this value (or greater) at infinite NH_4^+ concentrations, L must be ≥20. The difference between the active and less active enzyme forms and how NH_4^+ stabilizes the active form remains to be elucidated.

Since R181 appears to link the substrates to the protein via a hydrogen bond to L183 via the A and C nitrogens of the guanidinium group of R181, it is likely to play a role in closing the active site prior to catalysis. The isotope effect data are certainly consistent with this explanation (Tables 5 and 6 and Figure 5). The second NH_4^+, which likely binds as NH_3 to the B nitrogen position of the guanidinium group, may help to stabilize the closed enzyme form and facilitate catalysis in this manner. The wild-type enzyme activity is not affected by the presence of NH_4^+, but the enzyme is allosterically activated by fumarate and malate (*29*). Preliminary results suggest the R181Q mutant is activated by fumarate and malate in a manner qualitatively similar to that

[2] Personal communication.

of the wild-type enzyme (unpublished observation), thus suggesting that the activation of R181Q by NH_4^+ differs from the fumarate/malate activation.

Conclusions. Some of the functions attributed to R181 on the basis of three-dimensional structures are born out by this work. These functions can be summarized as follows.

(1) The large increases in the values of K_{malate} and $K_{ioxalate}$ support the role of R181 in binding substrate.

(2) In addition to its role in substrate binding, R181 affects catalysis by altering the rate of the precatalytic conformational change with no effect on decarboxylation.

(3) R181 also increases K_{iNADH} with little or no effect on K_{NAD}. Structural studies suggest an interaction between R181 and the nicotinamide ring of NADH, and the differential effect on binding the oxidized and reduced dinucleotide substrates and the suggested change in the partition ratio of oxaloacetate intermediate as NH_4^+ is added are consistent with a role for rotation of the nicotinamide ring into the malate site facilitating decarboxylation.

In addition, the activity of the R181Q mutant enzyme is rescued by 2 mol of ammonium ion per mole of enzyme active site. The high-affinity NH_4^+ likely occupies one of the guanidinium nitrogen sites **(**A position**)** and gives a regain of some of the binding affinity for malate, oxalate, and NADH, consistent with the roles of R181 suggested above. A second NH_4^+, likely binding as neutral NH_3, probably occupies the B position of the guanidinium nitrogen sites and appears to stabilize a more active enzyme conformation. Additional studies will be required to determine the exact location of the two ammonia-binding sites and the structural basis of their effects on binding and catalysis.

ACKNOWLEDGMENT

We thank Loan Nguyen for help in constructing the R181 mutant enzymes.

REFERENCES

1. Park, S.-H., Kiick, D. M., Harris, B. G., and Cook, P. F. (1984) Kinetic Mechanism in the Direction of Oxidative Decarboxylation for NAD-Malic Enzyme from *Ascaris suum*, *Biochemistry 23*, 5446−5453.
2. Karsten, W. E., and Cook, P. F. (1994) Stepwise versus Concerted Oxidative Decarboxylation Catalyzed by Malic Enzyme: A Reinvestigation, *Biochemistry 33*, 2096−2103.
3. Weiss, P. M., Gavva, S. R., Harris, B. G., Urbauer, J. C., Cleland, W. W., and Cook, P. F. (1991) Multiple isotope Effects with Alternative Dinucleotide Substrates as a Probe of the Malic Enzyme Reaction, *Biochemistry 30*, 5755−5763.
4. Karsten, W. E., Gavva, S. R., Park, S.-H., and Cook, P. F. (1995) Metal Ion Activator Effects on Intrinsic Isotope Effects for Hydride Transfer and Decarboxylation in the Reaction Catalyzed by the NAD-Malic Enzyme from *Ascaris suum*, *Biochemistry 34*, 3253−3260.
5. Grissom, C. B., and Cleland, W. W. (1986) Carbon Isotope Effects on the Metal Ion Catalyzed Decarboxylation of Oxaloacetate, *J. Am. Chem. Soc. 108*, 5582−5583.
6. Karsten, W. E., Hwang, C.-C, and Cook, P. F. (1999) α-Secondary Tritium Kinetic Isotope Effects Indicate Hydrogen Tunneling and Coupled Motion Occur in the Oxidation of L-Malate by NAD-Malic Enzyme, *Biochemistry 38*, 4398−4402.
7. Karsten, W. E., Liu, D., Rao, G. S. J., Harris, B. G., and Cook, P. F. (2005) A Catalytic Triad is Responsible for Acid-Base Chemistry in the *Ascaris suum* NAD-Malic Enzyme, *Biochemistry 44*, 3626−3635.
8. Coleman, D. E., Rao, G. S. J., Goldsmith, E. J., Cook, P. F., and Harris, B. G. (2002) Crystal Structure of the Malic Enzyme from *Ascaris suum* Complexed with Nicotinamide Adenine Dinucleotide at 2.3 Å Resolution, *Biochemistry 41*, 6928−6938.
9. Rao, G. S., Coleman, D. E., Karsten, W. E., Cook, P. F., and Harris, B. G. (2003) Crystallography Studies on *Ascaris suum* NAD-Malic Enzyme Bound to Reduced Cofactor and Identification of an Effector Site, *J. Biol. Chem. 278*, 38051−38058.
10. Tao, X., Yang, Z., and Tong, L (2003) Crystal Structures of Substrate Complexes of Malic Enzyme and Insights into the Catalytic Mechanism, *Structure 11*, 1141−1150.
11. Chang, G. G., and Tong, L. (2003) Structure and Function of Malic Enzymes, a New Class of Oxidative Decarboxylases, *Biochemistry 42*, 12721−12733.
12. Cervellati, C., Dallochio, F., Beramini, C. M., and Cook, P. F. (2005) Role of Methionine-13 in the Catalytic Mechanism of 6-Phosphogluconate Dehydrogenase from Sheep Liver, *Biochemistry 44*, 2432−2440.
13. Li, L., Zhang, L., and Cook, P. F. (2006) Role of the S128, H186, and N187 Triad in Substrate Binding and Decarboxylation in the Sheep Liver 6-Phosphogluconate Dehydrogenase Reaction, *Biochemistry 45*, 12680−12686.
14. Li, L., and Cook, P. F. (2006) The 2′-Phosphate of NADP is Responsible for Proper Orientation of the Nicotinamide Ring in the Oxidative Decarboxylation Reaction Catalyzed by Sheep Liver 6-Phosphogluconate Dehydrogenase, *J. Biol. Chem. 281*, 36803−36810.
15. Karsten, W. E., Chooback, L., Liu, D., Hwang, C.-C., Lynch, C., and Cook, P. F. (1999) Mapping the Active site Topography of the NAD-Malic Enzyme via Alanine-Scanning Site-Directed Mutagenesis, *Biochemistry 38*, 10527−10532.
16. Bradford, M. M. (1976) A Rapid and Sensitive Method for the Quantification of Microgram Quantities of Protein Utilizing the Principle of Protein-Dye Binding, *Anal. Biochem. 72*, 248−254.
17. Viola, R. E., Cook, P. F., and Cleland, W. W. (1979) Stereoselective Preparation of Deuterated Reduced Nicotinamide Adenine Nucleotide and Substrate by Enzymatic Synthesis, *Anal. Biochem. 96*, 334−340.
18. Smith, R M., and Martell, A. E. (1977) *Critical Stability Constants*, Vol. 3, Plenum Press, New York.
19. Smith, R M., and Martell, A. E. (1982) *Critical Stability Constants*, Vol. 5, Plenum Press, New York.
20. O'Leary, M. H. (1980) Determination of Heavy-Atom Isotope Effects on Enzyme-Catalyzed Reactions, *Methods Enzymol. 64*, 83−104.
21. Craig, N. (1957) Isotopic Standards for Carbon and Oxygen and Correction Factors for Mass-Spectrometric Analysis of Carbon Dioxide, *Geochim. Cosmochim. Acta 12*, 133−140.
22. Cleland, W. W. (1979) Statistical Analysis of Enzyme Kinetic Data, *Methods Enzymol. 63*, 103−138.
23. Cook, P. F., Blanchard, J. S., and Cleland, W. W. (1980) Primary and Secondary Deuterium Isotope Effects on Equilibrium Constants for Enzyme-Catalyzed Reactions, *Biochemistry 19*, 4853−4858.
24. Kiick, D. M., Harris, B. G., and Cook, P. F. (1986) Protonation Mechanism and Location of Rate-Determining Steps for the *Ascaris suum* Nicotinamide Adenine Dinucleotide-Malic Enzyme Reaction from Isotope effects and pH Studies, *Biochemistry 25*, 227−236.
25. Hsu, R. Y. (1982) Pigeon Liver Malic Enzyme, *Mol. Cell. Biochem. 43*, 3−26.
26. Rajapaksa, R., Abu-Soud, H., Raushel, F. M., Harris., B. G., and Cook, P. F. (1993) Pre-Steady-State Kinetics Reveal a Slow Isomerization of the Enzyme-NAD Complex in the NAD-Malic Enzyme Reaction, *Biochemistry 32*, 1928−1934.
27. Hermes, J. D., Roeske, C. A., O'Leary, M. H., and Cleland, W. W. (1982) Use of Multiple Isotope Effects to Determine Enzyme Mechanisms and Intrinsic Isotope Effects. Malic Enzyme and Glucose-6-phosphate Dehydrogenase, *Biochemistry 21*, 5106−5114.
28. Monod, J., Wyman, J., and Changeux, J. P. (1965) On the Nature of Allosteric Transitions: A Plausible Model, *J. Mol. Biol. 12*, 88−118.
29. Karsten, W. E., Pais, J. E., Jagannatha Rao, G. S., Harris, B. G., and Cook, P. F. (2003) *Ascaris suum* NAD-Malic Enzyme is Activated by L-Malate and Fumarate Binding to Separate Allosteric Sites, *Biochemistry 42*, 9712−9721.

BI701524Z